UDC 539.4

Brittle Mixed-Mode (I+II) Fracture: Application of the Equivalent Notch Stress Intensity Factor to the Cracks Emanating From Notches

H. El Minor,[a] M. Louah,[a] Z. Azari,[b] G. Pluvinage,[b] and A. Kifani[c]

[a] Laboratory of Applied Mechanics and Applied Technology, Rabat, Morocco

[b] L.F.M. Faculty of Sciences, University of Metz, Metz, France

[c] Laboratory of Mechanics and Physics of Materials, Rabat's Faculty of Sciences, University of Rabat, Rabat, Morocco

УДК 539.4

Хрупкий механизм разрушения смешанного типа I+II в трещинах, растущих из концентраторов напряжения: эквивалентный коэффициент интенсивности напряжений в концентраторе напряжения

Х. Эль Минор[а], М. Луах[а], З. Азари[б], Г. Плювинаж[б], А. Кифани[в]

[а] Лаборатория прикладной механики и технологии, Рабат, Марокко

[б] Лаборатория механической надежности, Метц, Франция

[в] Лаборатория механики и физики материалов, Рабат, Марокко

Исследуется зарождение трещины по смешанному механизму разрушения (типа I+II) в образцах кольцевого типа с внутренним надрезом. Предложен новый критерий для описания хрупкого разрушения смешанного типа I+II, в основу которого положен объемный подход, а базовым параметром служит касательное напряжение в надрезе. Предлагается в качестве параметра вязкости разрушения для смешанного механизма разрушения по типу I+II использовать предельное значение эквивалентного коэффициента интенсивности напряжений в надрезе.

Ключевые слова: хрупкий механизм разрушения смешанного типа I+II, влияние надреза, проблема угловой трещины, критерий максимального касательного напряжения, эффективное касательное напряжение, эффективная касательная протяженность, градиент относительного касательного напряжения, весовая функция, эквивалентный коэффициент интенсивности напряжений, вязкость разрушения.

Introduction. First studies of fracture mechanics were performed on precracked specimens loaded according to an elementary fracture mode I, because it is considered to be the most dangerous fracture mode. In reality, some situations result in a simultaneous presence of two modes of fracture: mode I (opening mode) and mode II (shear mode). In the latter case, no standardized test procedure exists. In recent years, a diversity of test conditions and types of specimens have been used in the fracture toughness investigations, which resulted in the development of

various mixed-mode fracture criteria, techniques of measuring threshold values of fatigue and determining the crack growth laws applicable to multiaxial stress situations. Some of these types of specimens have been presented and critically analyzed by Richard [1]. Recent investigations [2, 3] have shown that precracked circular ring specimens are well suited for the mixed-mode tests.

However, the above mentioned type of precracked specimens presents two inconveniences:

(i) manufacturing of these specimens is regarded to be time-consuming and expensive;

(ii) for very brittle materials, such as ceramics and high-strength steels, it is practically impossible to precrack specimens and, therefore, the use of a notched specimen is preferred instead.

At present, Creager's solution [4] is used for analytical representation of the stress intensity factor at the notch tip. This solution has been constructed by adding a geometrical correction factor to Irwin's solution [5]. The respective method is based on the assumption that the characteristic distance (or the process volume diameter) is equal to $\rho/2$ (where ρ is the notch radius). However, this procedure has a limited applicability.

Recently it has been proposed [6, 7] to characterize fracture conditions for a notched specimen by using the actual stress gradient at the notch root. This stress gradient can be characterized by a relationship different from the crack-tip stress gradient. This method has been used in the present work to determine fracture resistance in the applied mixed-mode (I+II) fracture using notched circular ring specimens. The toughness of high-strength steel 45SCD6 was defined by a critical equivalent notch stress-intensity factor. This approach is based on the generic stress of the "notch fracture mechanics."

Material and Specimens. Here we propose to check the validity of this fracture criterion using experimental results obtained from notched high-strength steel specimens subjected to compression loading. Stress distribution in the specimen has been determined using the finite element method.

The material studied is high-strength steel 45CDS6 according to the French standard. Its mechanical properties are listed in Table 1. Microanalysis of the material gives the following chemical composition: 0.45%C, 1.6%Si, 0.6%Mn, 0.6%Cr, and 0.25%Mo.

Table 1

Mechanical Properties of 45CDS6 Steel

Density (kg/m^3)	ν	A, %	E, MPa	$R_{p0.2}$, MPa	R_m, MPa	K_{Ic}, MPa$\sqrt{m}$
7800	0.28	2.8	210,065	1463	1662	97

Tests were performed using U-notched circular ring specimens (Fig. 1) with the external radius $R_e = 20$ mm, internal radius $R_i = 10$ mm, thickness $B = 7$ mm, and the notch length $a = 4$ mm. Different notch radii were obtained using a wire-cutting electrical discharge machine (EDM) and wires of different diameter. The notch-root radius was measured using a profile projector.

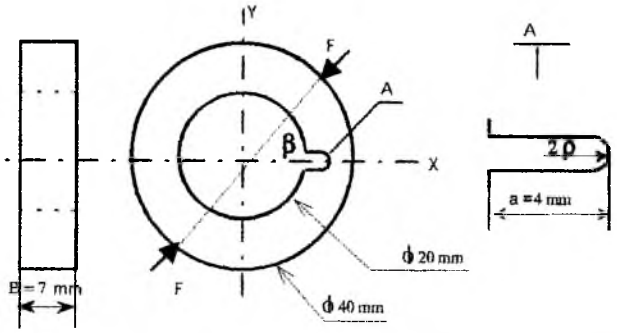

Fig. 1. U-notched circular ring specimen.

Fig. 2. Mechanical testing.

Definition of Different Fracture Modes:

a) $\beta = 0°$ – mode I [8];

b) $\beta = 33°$ – mode II [2] and [3];

c) $0° < \beta < 33°$ – mixed mode (I+II) fracture.

Mechanical Testing. Figure 2 shows a scheme of mechanical testing of notched specimens subjected to compression loading.

Experimental Procedure and Results. *Critical Load* P_c. Figure 3 shows evolution of the experimental critical load P_c versus the notch radius ρ and inclination angle β ($\beta = 0°$ in mode I, and $\beta = 33°$ in mode II). It is evident from Fig. 3 that the critical load P_c increases linearly with the notch radius ρ.

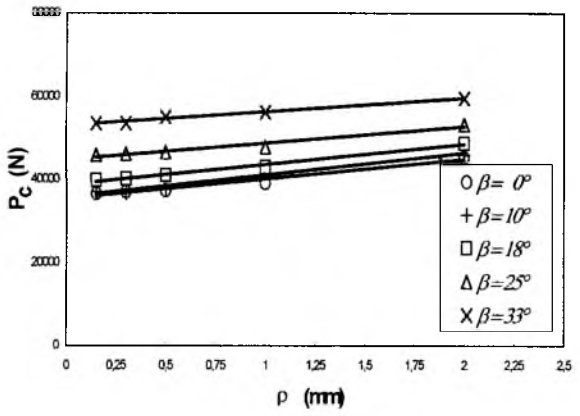

Fig. 3. Critical load P_c versus notch radius ρ for various inclination angles β.

Bifurcation Angle. The experimental values of the bifurcation angle θ_0 measured by an optical microscope (Fig. 4) are compared to the respective numerical values calculated using the maximum tangential stress criterion.

Mechanisms of Crack Initiation: "Volumetric Approach." According to an engineering approach, crack initiation occurs under whatever high stress concentration conditions and is defined as an appearance of a short crack detectable with a magnification of $\times 50$.

Figure 5 shows that blunted notches are characterized by the short crack mechanism, which means increasing of the crack growth rate after a decreasing period.

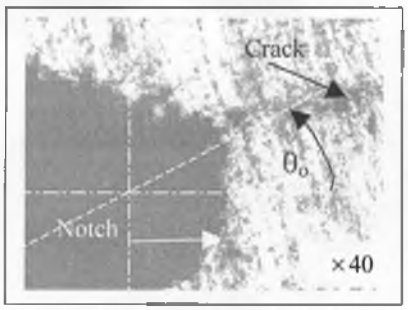

Fig. 4. Example of bifurcation angle for $\rho = 1$ mm and $\beta = 18°$.

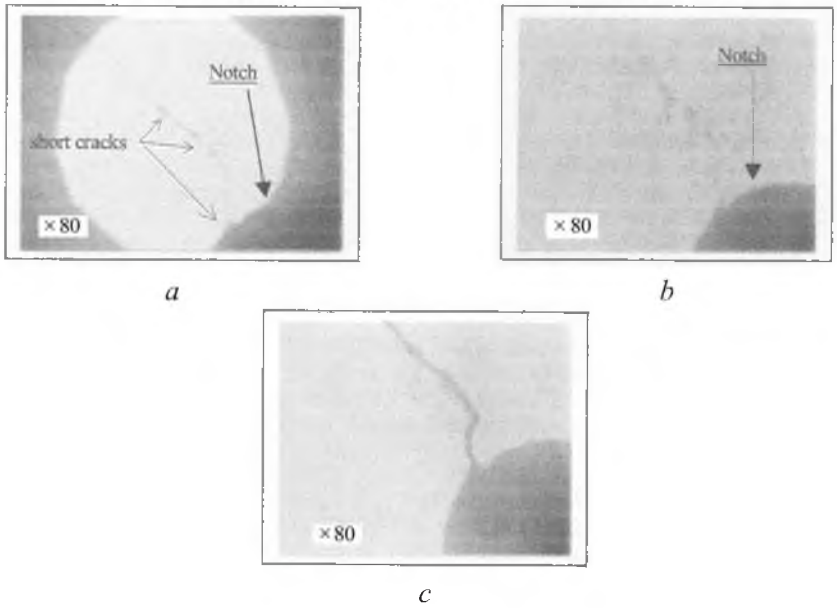

Fig. 5. Fracture micromechanism: (*a*) short crack mechanism; (*b*) evolution of microcracks; (*c*) crack growth.

The mechanisms of crack initiation have been described widely. These involve various intrusion and extrusion mechanisms in pure ductile metals or dislocation pile-up on inclusions, decohesion of the matrix and, finally, crack initiation.

The following two considerations support the notion that a certain physical volume is required for the crack initiation mechanisms to take place:

– The probability of crack initiation is proportional to the process volume, where the probability to find an initiation site (inclusion) is assumed to be uniform.

– Crack resistance is influenced by the specimen dimensions and relative stress gradient (i.e., the stress gradient divided by the stress value), which are dimensional parameters.

It has been proved that crack initiation mechanisms at the notch root cannot be explained by the spot approach, i.e., one of the key factors is the maximum local stress. We consider that the effective stress range acting in the crack-initiation process volume plays an important role in this respect.

Within this volume, the average stress is high enough to promote crack initiation, while the relative stress gradient is not too high, which makes all points within this volume to be sufficiently stressed (by the so-called "effective tangential stress"). The role of the relative stress gradient in the crack-initiation process has been mentioned previously by Buch [9].

Proposed Criterion for the Mixed-Mode Fracture Initiated from Notches: the Equivalent Notch Stress Intensity Factor. This criterion assumes that in mixed-mode (I+II) fracture crack initiation from notches is governed by the tangential stress.

For various notch radii and inclination angles we have determined the maximum tangential stress points over the notch contour. We have analyzed the distribution of tangential stresses at the notch tip according to this approach. This analysis shows a "pseudo singularity" stress distribution governed by the equivalent notch stress-intensity factor K_{eq}. We will show below that the critical values of this parameter can be used to determine the fracture toughness in mixed-mode (I+II) fracture.

Direction of the Maximum Tangential Stress at the Notch Tip. Finite element calculations (Castem 2000) have been used to determine the maximum tangential stress in all points of the notch contour. It is noteworthy that the respective direction varies linearly with the notch radius. This variation is given by the following correlations:

$$\theta_0 = A(\beta)\frac{\rho}{a} + B(\beta) \qquad \text{(in degrees)}, \tag{1}$$

where

$$A(\beta) = -0.0222\beta^2 + 1.4983\beta, \tag{2}$$

$$B(\beta) = -0.0456\beta^2 + 3.6178\beta. \tag{3}$$

In mode II ($\beta = 33°$) for $\rho = 0$: $\theta_0 = B(33°) = 70.39° \approx 70.5°$ (Sih and Erdogan [10]) or $\approx 70.33°$ (Stroh [11]).

The numerical values obtained according to the maximum tangential stress criterion [Eq. (1)] are compared to the experimental values measured by an optical microscope (Fig. 6).

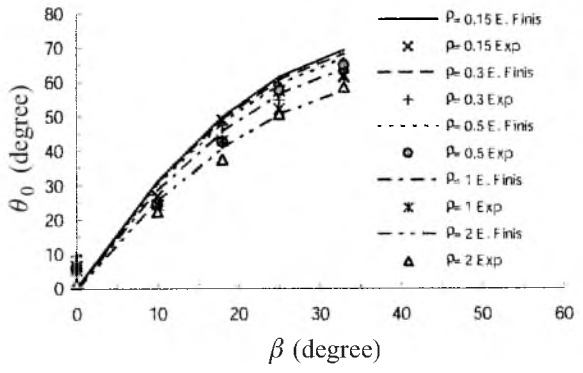

Fig. 6. Direction of the maximum tangential stress θ_0 versus the inclination angle β.

Figure 6 shows that the propagation of the angled crack θ_0 described according to the maximum tangential stress criterion correlates closely with the experimental data, and the above criterion can be used to predict the bifurcation angle for cracks emanating from notches.

Tangential Stress Distribution at the Notch Tip. In Fig. 7, we plot the evolution of the stress distribution at the notch tip versus the distance ρ according to the direction of the maximum tangential stress θ_0 (for $\rho = 0.5$ mm and $\beta = 18°$).

Figure 7 shows that the tangential stress $\sigma_{\theta\theta}$ is appreciably higher than σ_{rr}, σ_{zz}, and $\tau_{r\theta}$. This important difference is observed for various notch radii ρ and inclination angles β.

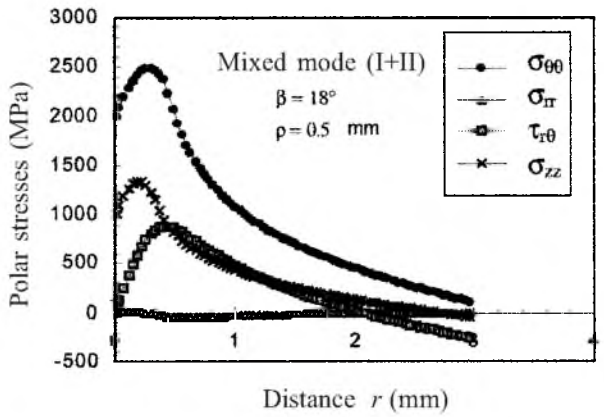

Fig. 7. Distribution of stresses $\sigma_{\theta\theta}$, σ_{rr}, σ_{zz}, and $\tau_{r\theta}$ at the notch tip.

We assume that the mixed-mode (I+II) notch-initiated fracture is governed by the tangential stress (while $\sigma_{\theta\theta}$ plays the major role in the cracking process). Further, we have studied this stress distribution according to the maximum tangential stress direction.

We have plotted the tangential stress distribution in a bilogarithmic graph (Fig. 8) according to the procedure described elsewhere [6, 7, 12].

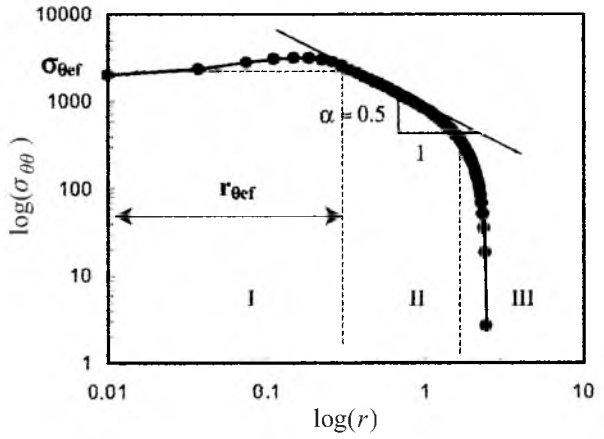

Fig. 8. Tangential stress distribution at the notch tip.

Zone I: "High-stress" region.

Zone II: "Pseudo singularity" stress distribution governed by the equivalent notch stress-intensity factor.

$$\sigma_{\theta\theta} = \frac{K_{eq\rho}}{\sqrt{2\pi r}}, \tag{4}$$

where $\sigma_{\theta\theta}$ is the tangential stress (MPa), r is the distance from the notch tip (mm), and $K_{eq\rho}$ is the equivalent notch stress intensity factor (MPa$\sqrt{\text{m}}$).

Zone III: "distant" region.

Effective Tangential Distance $r_{\theta ef}$. The upper limit of the "pseudo singularity" stress distribution has the following coordinates ($r_{\theta ef}$, $\sigma_{\theta ef}$), where $r_{\theta ef}$ is the effective tangential distance and $\sigma_{\theta ef}$ is the effective tangential stress.

By definition, the effective tangential distance is the diameter of the process volume assuming it has a cylindrical shape. A typical example of the tangential stress distribution is presented in Fig. 9. The relative tangential stress has also been plotted versus distance r.

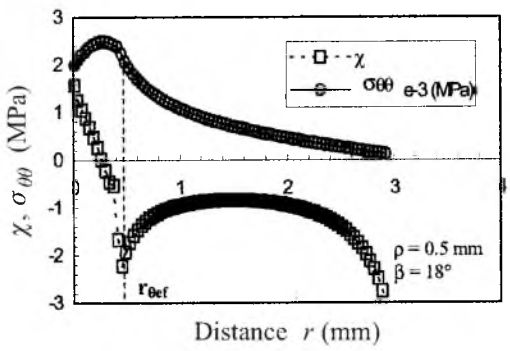

Fig. 9. Tangential stress distribution at the notch tip. Relative tangential stress gradient versus the distance. Determination of the effective tangential distance.

The relative tangential stress is defined as

$$\chi = \frac{1}{\sigma_{\theta\theta}(r)} \frac{d\sigma_{\theta\theta}(r)}{dr}. \tag{5}$$

The effective tangential distance can be determined using the following considerations:

1. According to [13], the effective tangential distance exceeds the plastic zone diameter $[R_p(\theta_0)]$.

2. The effective tangential distance is located in the stressed region, where the stress gradient is not too high.

Weight Function. All the stressed points in the process volume have a certain role in crack initiation from notches. This role is different for each point and depends both on the distance between this point and the notch, and on the stress gradient. We can define the ***weighted stress***, which takes into account these roles, as follows:

$$\sigma_{ij}^{*} = \sigma_{ij}\varphi(r, \chi), \tag{6}$$

where $\varphi(r, \chi)$ is the weight function. According to Weixing [14], this function is defined by the following relationship:

$$\varphi(r, \chi) = 1 - r\chi. \tag{7}$$

Effective Tangential Stress σ_{θ}^{ef}. The effective tangential stress is the stress, which corresponds to the effective distance of stress distribution. It is defined as

$$\sigma_{\theta}^{ef} = \frac{1}{r_{ef}} \int_{0}^{r_{ef}} \sigma_{\theta\theta}\varphi(r, \chi)dr. \tag{8}$$

This is the average value of the weighted tangential stress.

Critical Equivalent Notch Stress-Intensity Factor $K_{eq\rho}^{c}$ *and Fracture Toughness* K_{Ic}. In this section, we have determined the critical equivalent notch stress-intensity factor $K_{eq\rho}^{c}$ in mode I, mode II, and mixed mode (I+II) fracture. We compared its value to the fracture toughness K_{Ic} according to Jones [8], who considered a notch to be equivalent to a crack.

For circular ring specimens, Jones [8] expressed the fracture toughness K_{Ic} by the following relationship:

$$K_{Ic} = \frac{2.61P_c}{B\sqrt{R_0}}, \tag{9}$$

where $0.625 \le (a + R_i)/R_0 \le 0.845$ and $R_i/R_0 = 0.5$; $a \ge 0.4b$ $(b = R_0 - R_i)$, while 2.61 corresponds to the value of the geometrical correction and the critical load P_c.

According to [8], the fracture toughness K_{Ic} and the critical equivalent notch stress intensity factor $K_{eq\rho}^{c}$ have been determined from experimental and numerical results and presented, respectively, in Figs. 10 and 11 versus the notch radius ρ.

It is noteworthy that if the notch radius is less than ρ_c, the critical equivalent notch stress-intensity factor $K_{eq\rho}^{c}$ is practically constant and independent of both the notch radius and the inclination angle. The critical value of this parameter is nearly equal to the notch stress intensity factor $K_{I\rho}^{c}$ in mode I fracture:

$$K_{eq\rho}^{c} \approx K_{I\rho}^{c} \approx K_{Ic} \text{ (for } \rho < \rho_c = 0.75 \text{ mm)} \approx 97 \text{ MPa}\sqrt{\text{m}}. \tag{10}$$

However, according to [8], for $\rho > \rho_c = 0.75$ mm, the fracture toughness K_{Ic} exhibits a linear relationship with the notch radius ρ and is not an intrinsic material characteristic.

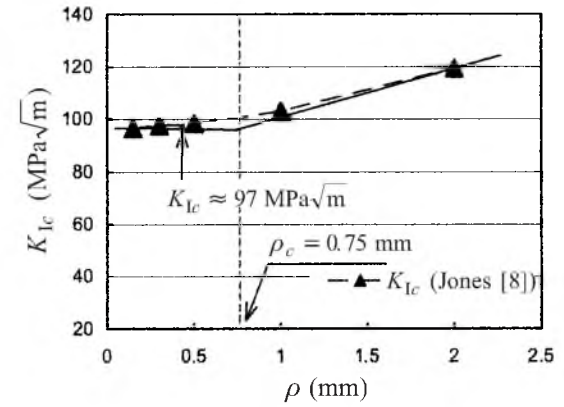

Fig. 10. The influence of the notch radius ρ on the fracture toughness K_{Ic}.

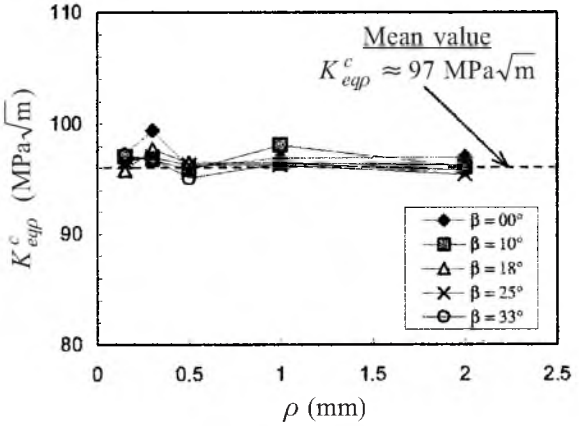

Fig. 11. The influence of the notch radius ρ on the critical equivalent-notch stress intensity factor $K^c_{eq\rho}$.

Mixed-Mode (I+II) Criterion Based on the Equivalent Notch Stress- Intensity Factor $K^c_{eq\rho}$. The tangential stress distribution at the notch tip can be described by two types of fracture criteria: global and local. In the case of a notch, there is no stress singularity at the crack tip, but the maximum stress is followed by a "pseudo singularity," where the stress distribution is governed by the equivalent notch stress-intensity factor.

Global Fracture Criterion. It is assumed that crack initiation occurs:

(i) in the direction perpendicular to the tangential stress when it reaches its maximum value;

(ii) when the equivalent notch stress-intensity factor $K^c_{eq\rho}$ reaches its critical value:

$$K^c_{eq\rho} = \sigma^c_{ef} \sqrt{2\pi r^c_{ef}} = K^c_{I\rho}. \tag{11}$$

Local Fracture Criterion (Volumetric Approach). The local fracture criterion is based on the following considerations: for physical reasons, a certain volume (called "effective volume") is required for the fracture process to occur. Within

this volume, the effective tangential stress can be considered as an average stress tangential weight, which takes into account the tangential stress distribution. This process volume can be described by the distance r_θ^{ef}, or the so-called "effective tangential distance" considering that the specimen thickness is constant and the process volume is cylindrical.

The crack initiation is assumed to occur when both the effective tangential stress σ_θ^{ef} and the effective tangential distance reach their critical values.

Conclusions. For brittle mixed-mode (I+II) fracture emanating from notches, the maximum tangential stress criterion, which is based on the effective tangential stress and the equivalent notch stress-intensity factor, agrees well with the experimental data and can be used to predict the bifurcation angle for cracks emanating from notches.

The volumetric approach envisages that the cracking process requires a physical volume to occur. The effective tangential stress acting in this volume (called the effective volume) is given by the value of the minimum relative tangential stress.

The results of this work and some other ones [6, 12, 15] indicate that this approach provides a relatively good description of the notch effect.

Р е з ю м е

Досліджується зародження тріщини за змішаним механізмом руйнування (типу I+II) в зразках кільцевого типу з внутрішнім надрізом. Запропоновано новий критерій для описання крихкого руйнування змішаного типу I+II, в основу якого покладено об'ємний підхід, а базовим параметром є дотичне напруження у надрізі. За параметр в'язкості руйнування для змішаного механізму руйнування за типом I+II пропонується використовувати граничне значення еквівалентного коефіцієнта інтенсивності напружень у надрізі.

1. H. A. Richard, "Specimens for investigating biaxial fracture and fatigue processes," in: *Biaxial and Multiaxial Fatigue*, Mechanical Engineering Publications (1989), pp. 217–229.
2. T. Tamine, C. Chehimi, T. Boukharouba, and G. Pluvinage, "Crack initiation in pure shear mode II," *Problems of Strength*, Special Publication, 71–79 (1996).
3. T. Tamine, *Amorçage de Fissures par Fatigue-Contact*, Thèse de Doctorat, Université de Metz, France (1994).
4. M. Creager and P. C. Paris, "Elastic field equations for blunt cracks with reference to stress corrosion cracking," *Int. J. Fract. Mech.*, **3**, 247–252 (1967).
5. G. R. Irwin, "Analysis of stresses and strains near the end of crack traversing a plate," *Trans. ASME, J. Appl. Mech.* (1957).
6. G. Pluvinage, "Rupture et fatigue amorcée à partir d'entailles – application du facteur d'intensité d'entaille," *Revue Franç. Mécan.*, No. 1, 53–61 (1997).

7. G. Pluvinage, *Notch Effect and Effective Stress in High-Cycle Fatigue*, Universite de Metz, France (1999).
8. A. T. Jones, "A radially cracked, cylindrical fracture toughness specimen," *Eng. Fract. Mech.*, **6**, 435–446 (1974).
9. A. Buch, "Analytical approach to size and notch-size effects in fatigue of aircraft material specimens," *Mat. Sci. Eng.*, **15**, 75–85 (1974).
10. G. C. Sih and F. Erdogan, "On the crack extension in plates under plane loading and transverse shear," *J. Basic Eng.* (1963).
11. G. Stroh, "La rupture des materiaux," in: D. Francois and L. Joly (Eds.), Masson and Co (1972).
12. N. Kadi, *Rupture par Fatigue des Arbres Entaillés et Clavetés*, Université de Metz, France (1997).
13. H. El Minor, *Rupture Fragile en Mode Mixte Amorcée à Partir d'Entaille*, Thèse de Doctorat, Université de Rabat, Morocco (in print).
14. Y. Weixing, "Stress field intensity approach for predicting fatigue life," *Int. J. Fract.*, **17**, No. 4, 245–251 (1995).
15. Z. Azari, N. Kadi, M. G. Jonaj, and G. Pluvinage, "Application of a new model proposal for the fatigue life prediction on notches and key-seats," *Int. J. Fatigue*, **21**, 53 (1999).

Received 19. 03. 2002